Proc. Natl. Acad. Sci. USA
Vol. 95, pp. 10559–10563, September 1998
Biochemistry

Activation of iron regulatory protein-1 by oxidative stress *in vitro*

KOSTAS PANTOPOULOS AND MATTHIAS W. HENTZE*

European Molecular Biology Laboratory, Meyerhofstrasse 1, D-69117 Heidelberg, Germany

Communicated by Helmut Beinert, University of Wisconsin–Madison, Madison, WI, July 1, 1998 (received for review November 28, 1997)

ABSTRACT **Iron regulatory protein-1 (IRP-1), a central cytoplasmic regulator of cellular iron metabolism, is rapidly activated by oxidative stress to bind to mRNA iron-responsive elements. We have reconstituted the response of IRP-1 to extracellular H_2O_2 in a system derived from murine B6 fibroblasts permeabilized with streptolysin-O. This procedure allows separation of the cytosol from the remainder of the cells (cell pellet). IRP-1 in the cytosolic fraction fails to be directly activated by addition of H_2O_2. IRP-1 activation requires the presence of a nonsoluble, possibly membrane-associated component in the cell pellet. The streptolysin-O-based *in vitro* system faithfully recapitulates characteristic hallmarks of IRP-1 activation by H_2O_2 in intact cells. We show that the H_2O_2-mediated activation of IRP-1 is temperature dependent and sensitive to treatment with calf intestinal alkaline phosphatase (CIAP). Although IRP-1 activation is unaffected by addition of excess ATP or GTP to this *in vitro* system, it is negatively affected by the nonhydrolyzable nucleotide analogs adenylyl-imidodiphosphate and guanylyl-imidophosphate and completely blocked by ATP-γS and GTP-γS. The *in vitro* reconstitution of this oxidative stress-induced pathway has opened a different avenue for the biochemical dissection of the regulation of mammalian iron metabolism by oxidative stress. Our data show that H_2O_2 must be sensed to stimulate a pathway to activate IRP-1.**

The coordinate posttranscriptional regulation of cellular iron metabolism in higher eukaryotes involves interactions between two iron regulatory proteins, IRP-1 and IRP-2, with iron-responsive elements (IREs), their cognate binding sites in the untranslated regions of several mRNAs (reviewed in refs. 1 and 2). These include, among others, the mRNAs encoding the transferrin receptor and ferritin H- and L- subunits. Iron deficiency and nitric oxide induce high affinity binding of IRPs to IREs. As a result of IRE/IRP interactions, transferrin receptor mRNA is stabilized, leading to increased iron uptake, and ferritin synthesis is repressed, associated with a concomitant reduction in iron storage. In most mammalian cells, IRP-1 is more abundant than IRP-2, and can therefore be considered as the major posttranscriptional regulator of cellular iron metabolism.

IRP-1 and IRP-2 display 57% identity and 79% similarity, and both belong to the family of Fe–S isomerases (3), which also includes mitochondrial aconitase. However, their RNA-binding activities are regulated by distinct posttranslational mechanisms. Whereas IRP-2 is controlled at the level of protein stability, regulation of IRP-1 involves Fe–S cluster assembly/disassembly (reviewed in refs. 1, 2, and 4–6). In iron-loaded cells, IRP-1 assembles a cubane 4Fe–4S cluster, which renders it functionally inactive for IRE binding, but active as a cytosolic aconitase, whereas disassembly of the cluster as a result of iron deficiency yields apoIRP-1, the active RNA-binding form.

In the last few years, we and others have demonstrated that IRP-1 (but not IRP-2) is rapidly activated by extracellular H_2O_2 to bind IREs (7–10). This finding has established a distinctive regulatory connection between the control of iron metabolism and responses to oxidative stress. Considering that iron toxicity is heavily based on Fenton chemistry, i.e., the generation of highly reactive hydroxyl radicals from the reaction of H_2O_2 with Fe^{2+} (11), this regulatory link is particularly important to understand. In addition, the response of IRP-1 to oxidative stress poses a challenge to unravel the mechanism that underlies the 4Fe–4S cluster disassembly. In accordance with the reported sensitivity of the 4Fe–4S cluster in bacterial and mammalian mitochondrial aconitases toward $O_2^{\cdot-}$ (12, 13), a plausible possibility would imply that the 4Fe–4S cluster of IRP-1 is liable to direct chemical modification by reactive oxygen intermediates (14, 15), finally resulting in disassembly. However, even though this model could account for the fast kinetics of IRP-1 activation by H_2O_2, recent data suggest that a profound increase in intracellular H_2O_2 levels is not sufficient to activate IRP-1 (16). Furthermore, a bolus of exogenous H_2O_2, which is rapidly degraded, elicits IRP-1 activation without a detectable increase in intracellular H_2O_2 levels (16). The activation kinetics under these conditions are biphasic, and the presence of a threshold concentration of H_2O_2 is only required in the early phase (0–15 min) of the treatment (9, 16). In contrast to the profound effects on IRP-1 following exposure of intact cells to H_2O_2, treatment of cytoplasmic cell extracts with H_2O_2 fails to activate IRP-1 (7, 8). Moreover, treatment of rat liver lysates or recombinant IRP-1 with xanthine and xanthine oxidase, which yields $O_2^{\cdot-}$ and H_2O_2, even results in a decrease in IRE-binding activity (17). Taken together, these data provide indirect evidence that the rapid activation of IRP-1 by extracellular H_2O_2 in intact cells is mediated by a signaling pathway.

The role of reactive oxygen intermediates in eukaryotic signaling networks has recently received much attention, because an increasing number of gene regulatory and enzymatic activities have been revealed to be modulated by oxidative stress; for example, the transcription factor NF-κB (18), the early response genes c-*fos*, c-*jun*, and *egr*-1 (19), the *Saccharomyces cerevisiae* metallothionein gene CUP1 (20), and several kinases, such as $p56^{lck}$ (21), SOK-1 (22), and protein kinase C (23). These stress-response pathways have been difficult to examine biochemically because of the lack of appropriate *in vitro* systems. Here, we have established an *in vitro* system based on permeabilized cells that faithfully reconstitutes the activation of IRP-1 by H_2O_2. By employing this system, we have identified important characteristics of the activation pathway and, for the first time, provide direct

The publication costs of this article were defrayed in part by page charge payment. This article must therefore be hereby marked "*advertisement*" in accordance with 18 U.S.C. §1734 solely to indicate this fact.

Abbreviations: IRE, iron-responsive element; IRP, iron regulatory protein; SLO, streptolysin-O; EMSA, electrophoretic mobility shift assay; 2-ME, 2-mercaptoethanol; CIAP, calf intestinal alkaline phosphatase; AMP-PNP, adenylyl-imidodiphosphate; GMP-PNP, guanylyl-imidodiphosphate.

*To whom reprint requests should be addressed. e-mail: hentze@embl-heidelberg.de.

evidence for a signaling mechanism leading to H_2O_2-mediated IRP-1 activation.

MATERIALS AND METHODS

Materials. Recombinant streptolysin-O (SLO) was purchased from S. Bhakdi (Institute of Medical Microbiology, University of Mainz, Germany). Glucose oxidase, catalase, herbimycin A, rapamycin, chelerythrine, staurosporine, H7, phorbol 12-myristate 13-acetate, ATP-γS, and GTP-γS were from Sigma; genistein and okadaic acid from LC Laboratories; and CIAP, adenylyl-imidodiphosphate (AMP-PNP), and guanylyl-imidodiphosphate (GMP-PNP) from Boehringer Mannheim. SB-203580 was a generous gift from J. C. Lee (SmithKline Beecham). A bioluminescence ATP assay kit (CLS II) was purchased from Boehringer Mannheim, and ATP measurements were performed according to the supplier's instructions.

Permeabilization of B6 Fibroblasts with SLO. B6 fibroblasts were grown as described (24). Before the permeabilization, cells were washed twice with PBS, harvested by scraping with a rubber policeman, pelleted by gentle centrifugation (1,000 × *g* for 5 min in a Sorvall RT6000B table top centrifuge), and resuspended in SLO buffer (25 mM Hepes·KOH, pH 7.4/115 mM potassium acetate/2.5 mM magnesium acetate/10 mM glucose). Cells were treated with 0.5 μg/ml SLO for 10 min on ice, pelleted by gentle centrifugation (1,000 × *g* for 5 min), resuspended in SLO buffer (10^7 cells per ml), and tumbled at 37°C for 20 min. Permeabilization was >95%, as assessed by trypan blue exclusion.

Treatment with an H_2O_2-Generating System. SLO-permeabilized cells were treated with H_2O_2, generated enzymatically by glucose oxidase and glucose. The suspension was tumbled at 37°C for the indicated times. The steady-state concentration of H_2O_2 in the suspension ($k_{GO} = 1.4 \times 10^{-8}$ M·s^{-1}), was estimated to be ≈50 μM by taking into account degradation by cellular activities (16). This was also confirmed by a semiquantitative peroxide test (Merckoquant) from Merck. All reactions were stopped by addition of excess catalase ($k_{cat} = 695$ s^{-1}) and the cells were pelleted by centrifugation. Where indicated, the cell pellets remaining after SLO permeabilization and centrifugation were solubilized in 1% Triton X-100, 40 mM KCl, and 25 mM Tris·Cl (pH 7.4) (cytoplasmic lysis buffer), and centrifuged (10,000 × *g* for 5 min).

Electrophoretic Mobility Shift Assay (EMSA). EMSAs with a radiolabeled human ferritin H-chain IRE probe were performed exactly as described (24). IRE/IRP-1 complex formation was quantitated by phosphorimaging. The data shown in Figs. 1–4 are representative of at least three independent experiments.

RESULTS

***In Vitro* Reconstitution of IRP-1 Activation by H_2O_2.** The previously observed failure to recapitulate the H_2O_2-mediated activation of IRP-1 *in vitro* (7, 8, 17) suggests that essential, possibly noncytoplasmic components were either missing from the extracts or inactivated. We thus explored more gentle preparative conditions by employing permeabilized rather than completely lysed cells. In the course of these exploratory experiments, the best results were obtained using SLO, a *S. aureus* toxin, which binds to cholesterol in the plasma membrane, aggregates, and forms transmembrane pores of up to 30 nm diameter (25). Permeabilization with SLO allows diffusion of soluble cell constituents and separation of the cytosol from the cell pellet by centrifugation (Fig. 1*A*).

The IRP-1 response to H_2O_2 was first assessed in suspensions of SLO-permeabilized and intact control B6 fibroblasts (Fig. 1*B*). After treatment with H_2O_2 for 1 hr, IRE-binding

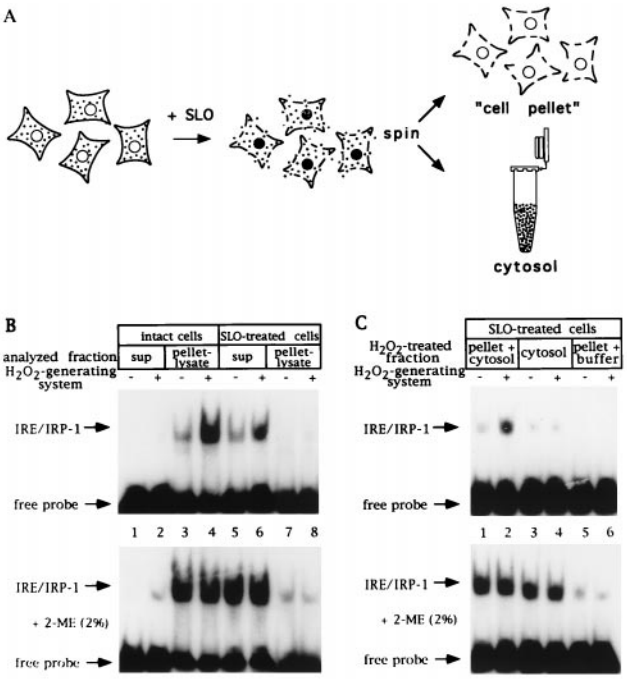

FIG. 1. A cell-free assay for IRP-1 activation by H_2O_2 based on SLO-permeabilized cells; requirement for nonsoluble factor(s). (*A*) Schematic representation of the SLO-permeabilization procedure. (*B*) Fibroblasts (10^7 control and 10^7 SLO-permeabilized B6) were suspended in 250 μl SLO buffer, tumbled for 20 min at 37°C, and treated with an H_2O_2-generating system (see *Materials and Methods*) for 1 hr. Following centrifugation, 10 μl of supernatants (2.5 μg/μl) and pellet lysates (25 μg protein) were analyzed by EMSA with 25,000 cpm radiolabeled IRE probe without (*Upper*) or with (*Lower*) 2% 2-ME. Lanes: 1, 2, 5, and 6, supernatants; 3, 4, 7, and 8, pellet lysates (in cytoplasmic lysis buffer) of intact and SLO-permeabilized cells treated without or with H_2O_2. (*C*) Fibroblasts (10^7 B6) were permeabilized with SLO as in *B*. Cytosol was separated by gentle centrifugation (supernatant) and cell pellets were washed twice with SLO buffer. Cytosol alone and cell pellets, mixed with one cytosol equivalent or resuspended in buffer, were treated, or not, with H_2O_2 for 1 hr. Following centrifugation, 10 μl of supernatants (2.5 μg/μl) were analyzed by EMSA with 25,000 cpm radiolabeled IRE probe without (*Upper*) or with (*Lower*) 2% 2-ME. Lanes: 1 and 2, cell pellet mixed with cytosol; 3 and 4, cytosol alone; 5 and 6, cell pellets resuspended in buffer, treated without or with H_2O_2. Positions of IRE/IRP-1 complexes and excess free probe are indicated by arrows.

activity in the supernatants and pellet-derived lysates was analyzed by EMSA. Although, as expected, IRP-1 activity is detected in the lysate prepared from the pellet of intact control cells (compare lanes 1 and 2 with lanes 3 and 4), IRP-1 is predominantly found in the supernatant from SLO-permeabilized cells (compare lanes 5 and 6 with lanes 7 and 8). Treatment of SLO-permeabilized cells with H_2O_2 activates IRP-1, as observed in the intact cells (7-fold induction in intact cells, lanes 3 and 4, and 4-fold induction in permeabilized cells, lanes 5 and 6). In Fig. 1*B* (*Lower*), identical samples were treated with 2% 2-mercaptoethanol (2-ME) to completely activate IRE binding of dormant IRP-1 *in vitro* (26), and subsequently subjected to EMSA. This result indicates that more than 95% of cytoplasmic IRP-1 is released from the cell pellet after permeabilization with SLO (compare lanes 5 and 6 with lanes 7 and 8) and, in addition, serves as a control for the equal loading of activatable IRP-1 onto the gel. We conclude that permeabilization of B6 fibroblasts with SLO is quantitative, and that treatment of the permeabilized cells with H_2O_2 leads to the activation of IRP-1.

We next tested whether the SLO-derived cytosol by itself contained all necessary components for the activation of IRP-1

by H_2O_2. B6 fibroblasts were permeabilized with SLO, the cytosol separated by centrifugation, and the cell pellet washed and resuspended in SLO buffer. Cytosol and the resuspended cell pellet were each divided into four aliquots. Two of the aliquots were treated separately with or without H_2O_2, whereas the other aliquots of cells and cytosol were mixed at a ratio of 1:1 to receive or not receive H_2O_2. After 1 hr, equal volumes of the supernatants were recovered by centrifugation and analyzed for IRE binding by EMSA (Fig. 1*C*). Although treatment of the cytosol alone with H_2O_2 has no effect on IRP-1 activity, combination of the cytosolic with the cell pellet fraction suffices to allow IRP-1 activation by H_2O_2 (compare lanes 1 and 2 with lanes 3 and 4). This result represents an *in vitro* reconstitution of IRP-1 activation by H_2O_2, and indicates that nonsoluble cell factors are indispensable to sense, mediate, and/or execute the H_2O_2 signal. By contrast, when SLO-derived cytosol or detergent-derived cytoplasmic cell extracts were treated with concentrated (at least 50-fold excess compared with our standard assay conditions) preparations of the glucose/glucose oxidase H_2O_2-generating system, we observed a reversible (with 2-ME) inactivation of IRP-1, consistent with previous findings (17) (data not shown). These conditions yield supraphysiological concentrations of H_2O_2.

To assess whether the effects shown in Fig. 1 faithfully reflect the *in vivo* response of IRP-1 to H_2O_2, we compared the kinetics of IRP-1 activation by H_2O_2 in intact and SLO-permeabilized cells. Identical to what was found *in vivo* (7–9, 16), treatment of SLO-permeabilized B6 fibroblasts with H_2O_2 results in a partial (2.7-fold) activation of IRP-1 after 15 min (Fig. 2*A*, lane 4) and in a complete activation within 30–60 min (4.2- and 7-fold, lanes 5 and 6). No significant activation is observed during the first 10 min of treatment (lanes 2 and 3), whereas incubations with H_2O_2 for up to 2 hr did not result in a higher degree of IRP-1 activation (data not shown). Simultaneous addition of an excess of catalase together with the H_2O_2-generating system to prevent H_2O_2 accumulation, followed by incubation at 37°C for 60 min, completely abolishes IRP-1 activation (compare lane 6 with lane 7). Thus, the observed activation of IRP-1 in the SLO-permeabilized cells depends on H_2O_2 and, moreover, follows kinetics identical to those observed in intact cells. Indeed, by analogy to intact cells, this activation is biphasic and only requires the transient presence of H_2O_2 for an induction phase of 15 min. When excess catalase is added to terminate a 5–15 min pulse with H_2O_2 and the suspension is subsequently chased at 37°C for up to 1 hr, inactive IRP-1 is partially induced 3.6- and 5-fold (compare lanes 1–3 in Fig. 2 *A* and *B*), and partially activated IRP-1 is completely activated (6.8-fold) in the absence of H_2O_2 (compare lanes 1 and 4 in Fig. 2 *A* and *B*). This again mirrors precisely our previous findings with intact cells (9, 16). Interestingly, the presence of nonsoluble factors appears to contribute to both phases of IRP-1 activation by H_2O_2, as the execution of IRP-1 activation after an initial pulse with H_2O_2 is clearly less evident in the SLO cytosol (Fig. 2*C*, lanes 2–4, induction 1-, 1.5-, and 2.8-fold, respectively).

Activation of IRP-1 by H_2O_2 Is Temperature-Dependent. The above data support the hypothesis that the transient presence of H_2O_2 at a concentration above a critical threshold triggers a stress response in both intact and SLO-permeabilized cells, which results in activation of IRP-1. To assess whether this pathway is temperature-sensitive, SLO-permeabilized cells were treated with a bolus of 0.5 or 1 mM H_2O_2 for 1 hr at 37°C or at 4°C. To prevent the rapid degradation of H_2O_2 by cellular catalase, cells were pretreated with 50 mM of the catalase inhibitor 3-amino-1,2,4-triazole 2 hr before permeabilization. Following such treatment, catalase activity was previously found significantly (70%) inhibited in a detergent-derived B6 cell lysate (16). Analysis of IRE-binding activity by EMSA reveals that activation of IRP-1 by H_2O_2 only occurs at 37°C, and not at 4°C (Fig. 3*A*), suggesting that this is a temperature- and possibly energy-dependent process.

IRP-1 Activation by H_2O_2 Is Inhibited by CIAP Treatment and by Nucleotide Triphosphate Analogs. We next addressed whether incubation with CIAP has an influence on IRP-1 activation by H_2O_2 in SLO-permeabilized cells. Following permeabilization, cells were pretreated with the enzyme for 30 min before generation of H_2O_2. Under these conditions, IRP-1 activation by H_2O_2 is inhibited (Fig. 3*B*), indicating that the pathway may involve phosphorylation steps and/or require ATP. Determination of the ATP concentration in the supernatants revealed that the treatment with CIAP results in a 90% reduction of ATP levels, from ≈10 μM in control to ≈1 μM in phosphatase-treated permeabilized cells.

Many signaling cascades require ATP and GTP as sources of energy and/or as phosphate group donors in phosphotransfer reactions. To examine the role of these nucleotide triphosphates in the activation of IRP-1 by H_2O_2, we employed ATP, GTP, and their analogs ATP-γS and GTP-γS and AMP-PNP and GMP-PNP. ATP-γS and GTP-γS are hydrolyzed very slowly by phosphatases and ATPases or GTPases. In addition, ATP-γS serves as a substrate for kinases to yield thiophosphorylated proteins that are resistant to protein phosphatases. The imidodiphosphate analogs AMP-PNP and GMP-PNP are nonhydrolyzable between the β and the γ phosphorus atoms. Treatment of SLO-permeabilized cells with 1 mM ATP exhibits little effect on IRP-1 activation by H_2O_2 (Fig. 3*C*, lanes 1–4). However, 1 mM AMP-PNP inhibits IRP-1 activation by ≈15% (lanes 7 and 8), whereas 1 mM ATP-γS completely

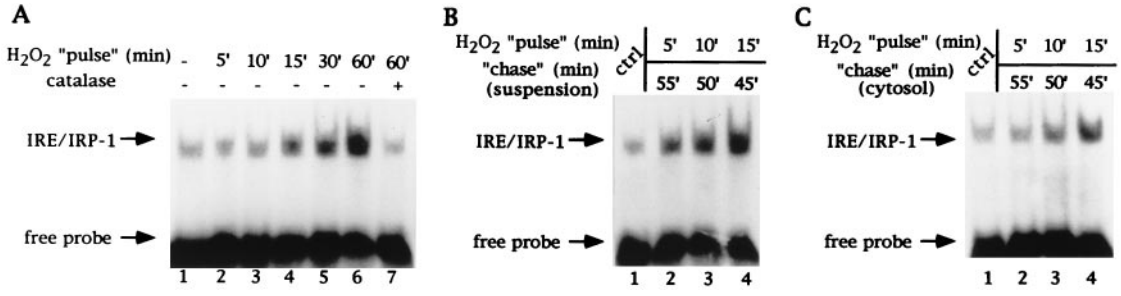

FIG. 2. Kinetic analysis of IRP-1 activation by H_2O_2 in SLO-permeabilized cells. (*A*) Fibroblasts (10^7 B6) were permeabilized with SLO as in Fig. 1*B* and treated with a pulse of H_2O_2 for the indicated times at 37°C. H_2O_2 was generated enzymatically and reactions were stopped by addition of excess catalase (k_{cat} = 695 s^{-1}) as described. One-third of the samples were centrifuged, supernatants were chilled on ice for up to 1 hr, and 10 μl (2.5 μg/μl) were analyzed by EMSA with 25,000 cpm radiolabeled IRE probe. Lanes: 1, untreated control; 2–6, treatment with H_2O_2 for 5, 10, 15, 30, and 60 min; 7, simultaneous treatment with H_2O_2 and excess catalase. (*B*) One-third of the samples corresponding to lanes 1–4 in *A* were tumbled at 37°C for up to 1 hr. Following centrifugation, 10 μl of supernatants (2.5 μg/μl) were analyzed by EMSA as in *A*. (*C*) One-third of the samples corresponding to lanes 1–4 in *A* were centrifuged. Supernatants were incubated at 37°C for up to 1 hr and 10 μl (2.5 μg/μl) were analyzed by EMSA as in *A*. Positions of IRE/IRP-1 complexes and excess free probe are indicated by arrows. Analysis of the same extracts in the presence of 2% 2-ME confirmed equal loading (not shown).

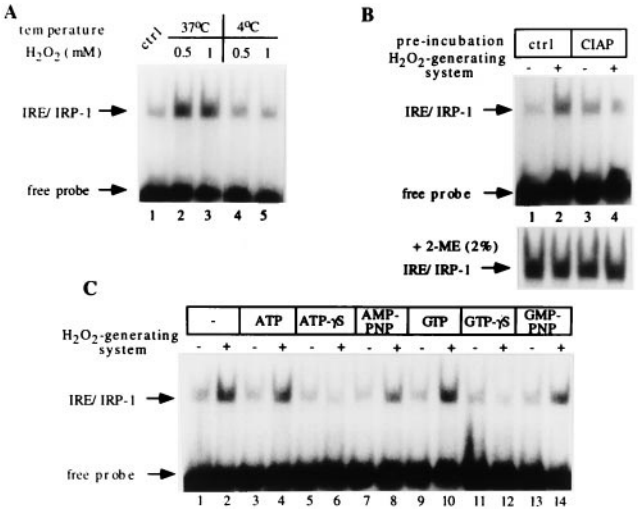

FIG. 3. IRP-1 activation by H_2O_2 in SLO-permeabilized cells is temperature and phosphorylation dependent. (*A*) Fibroblasts (10^7 B6), pretreated for 2 hr with 50 mM 3-amino-1,2,4-triazole, were permeabilized with SLO as in Fig. 1*B* and treated for 1 hr with a bolus of H_2O_2, either at 37°C or at 4°C. Following addition of catalase (k_{cat} = 695 s^{-1}) and centrifugation, 10 μl of supernatants (2.5 $\mu g/\mu l$) were analyzed by EMSA with 25,000 cpm radiolabeled IRE probe. Lanes: 1, untreated control; 2 and 3, treatment with 0.5 or 1 mM H_2O_2 at 37°C; 4 and 5, treatment with 0.5 or 1 mM H_2O_2 at 4°C. (*B*) Fibroblasts (10^7 B6) were permeabilized with SLO as in Fig. 1*B*, pretreated without or with 20 units CIAP for 20 min at 37°C, and subsequently without or with H_2O_2 for 1 hr. Following centrifugation, 10 μl of supernatants (2.5 $\mu g/\mu l$) were analyzed by EMSA with 25,000 cpm radiolabeled IRE probe. Lanes: 1 and 2, control pretreated cells treated without or with H_2O_2; 3 and 4, cells pretreated with CIAP and treated without or with H_2O_2. (*Lower*) Extracts were additionally treated with 2% 2-ME. Only the IRE/IRP complexes are shown. (*C*) Fibroblast (10^7 B6) were permeabilized with SLO as in Fig. 1*B* and treated with H_2O_2 for 1 hr in the presence of the indicated nucleotide triphosphates. Following centrifugation, 10 μl of supernatants (2.5 $\mu g/\mu l$) were analyzed by EMSA with 25,000 cpm radiolabeled IRE probe. Lanes: 1 and 2, control cells; 3 and 4, treatment with 1 mM ATP, 5 and 6, 1 mM ATP-γS; 7 and 8, 1 mM AMP-PNP; 9 and 10, 1 mM GTP; 11 and 12, 1 mM GTP-γS; 13 and 14, 1 mM GMP-PNP without or with H_2O_2, respectively. The positions of IRE/IRP-1 complexes and excess free probe are indicated by arrows. Analysis of the same extracts in the presence of 2% 2-ME confirmed equal loading (not shown).

abolishes this response (lanes 5 and 6). Similarly, whereas 1 mM GTP fails to antagonize IRP-1 activation by H_2O_2 (lanes 9 and 10), treatments with 1 mM GMP-PNP or with 1 mM GTP-γS result in partial (≈15%) or complete (lanes 11 and 12) inhibition of IRP-1 activation, respectively.

In all experiments, permeabilization of cells and treatments with H_2O_2 were performed in SLO buffer, which contains 2.5 mM Mg^{2+}. As many kinases catalyze phosphorylation reactions by Mg^{2+}-dependent mechanisms, we wondered whether chelation of Mg^{2+} may affect the activation of IRP-1 by H_2O_2. Indeed, treatment of SLO-permeabilized cells with EDTA inhibits IRP-1 activation by H_2O_2, whereas treatment with EGTA, which preferentially chelates Ca^{2+}, exhibits no effect (compare 4-fold IRP-1 activation by H_2O_2 in control and EGTA-treated cells with 1.3-fold activation in EDTA-treated cells, Fig. 4*A*). Interestingly, a very potent inhibitor of the stress-response pathway was identified in the metabolic poison sodium azide. Treatment of SLO-permeabilized cells with ≥10 μM sodium azide completely blocks activation of IRP-1 by H_2O_2 (Fig. 4*B*). Since sodium azide (even in millimolar concentrations) does not prevent generation of H_2O_2 by glucose oxidase and glucose (ref. 27, also confirmed with the semiquantitative peroxide test Merckoquant), this result suggests that it inhibits components involved in activation of

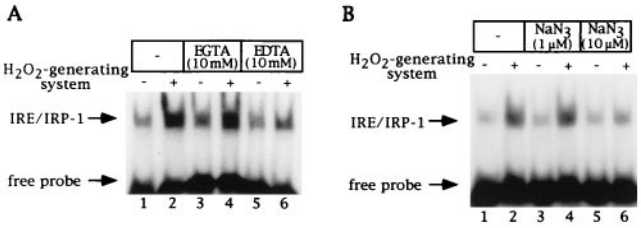

FIG. 4. H_2O_2-mediated activation of IRP-1 in SLO-permeabilized cells is inhibited by EDTA and sodium azide. (*A*) Fibroblasts (10^7 B6) were permeabilized with SLO as in Fig. 1*B* and treated without or with H_2O_2 for 1 hr in the presence of EGTA or EDTA. Following centrifugation, 10 μl of supernatants (2.5 $\mu g/\mu l$) were analyzed by EMSA with 25,000 cpm radiolabeled IRE probe. Lanes: 1 and 2, control cells; 3 and 4, treatment with 10 mM EGTA; 5 and 6, treatment with 10 mM EDTA, without or with H_2O_2, respectively. (*B*) Fibroblasts (10^7 B6) were permeabilized with SLO as in Fig. 1*B* and treated without or with H_2O_2 for 1 hr in the presence of sodium azide. Following centrifugation, 10 μl of supernatants (2.5 $\mu g/\mu l$) were analyzed by EMSA with 25,000 cpm radiolabeled IRE probe. Lanes: 1 and 2, control cells; 3 and 4, treatment with 1 μM sodium azide; 5 and 6, treatment with 10 μM sodium azide, without or with H_2O_2, respectively. These concentrations of sodium azide do not inhibit catalase activity in cell extracts (S. Mueller, personal communication). The positions of IRE/IRP-1 complexes and excess free probe are indicated by arrows. Analysis of the same extracts in the presence of 2% 2-ME confirmed equal loading (not shown).

IRP-1 by H_2O_2. The concentration of ATP in supernatants of both control and sodium azide-treated permeabilized cells was found to be ≈10 μM. This implies that in this concentration range, sodium azide does not diminish ATP levels in SLO-permeabilized cells.

DISCUSSION

We have biochemically characterized the cellular activation of IRP-1 by H_2O_2 by using a reconstituted *in vitro* system based on SLO-permeabilized cells. Previous attempts to do so in cytoplasmic cell lysates have failed (7, 8) or even resulted in IRP-1 inactivation (data not shown and ref. 17). Oxidative inactivation of IRP-1 *in vitro* by diamide has also been reported (26). In this paper we show (Fig. 2) that the SLO-based system faithfully recapitulates the H_2O_2-mediated activation of IRP-1 in intact cells (7–10, 16), and that cytosol lacks a component(s) that is essential for this response. In SLO-permeabilized B6 fibroblasts, at least one of these components is not soluble and remains associated with the cell pellet. The exact subcellular localization of these activating components remains to be identified. It is possible that these are expressed in, or in close association with, intracellular organelles. However, our previous data do not seem to favor this interpretation; measuring the fate of extracellular H_2O_2 and probing the relative levels of intracellular H_2O_2 with a redox-sensitive fluorescent dye suggested that only extracellular H_2O_2 elicits the typical rapid biphasic activation of IRP-1 (16). These findings and the data presented here raise the intriguing possibility that the nonsoluble activating factor may represent a plasma membrane-associated H_2O_2 sensor. Such a factor could function either as a transmembrane or as a membrane-associated H_2O_2 receptor required to activate IRP-1 by means of an oxidative stress-response signaling pathway, which is temperature and possibly energy dependent (Fig. 3). This pathway appears to require Mg^{2+} and to be sensitive to treatment with CIAP or sodium azide (Figs. 3 and 4). The quantitative differences of γ-S- and imidodiphosphate- nucleotide analogs in the inhibition of IRP-1 activation by H_2O_2 (Fig. 3*C*) suggest that the γ-S analogs not only compete for ATP and GTP hydrolysis but may also serve as substrates for the thiophosphorylation of proteins. Taken together, IRP-1 activation by H_2O_2 in SLO-

permeabilized cells appears to require ATP and GTP, reflecting an energy requirement of this process and/or the involvement of phosphorylation/dephosphorylation steps.

These findings provide the most direct evidence to date that IRP-1 activation by H_2O_2 involves cellular signaling events. They also lay the foundation for a further detailed biochemical and molecular characterization of the involved factor(s). Moreover, the SLO-based *in vitro* system should also allow a detailed analysis of whether activation involves the phosphorylation of IRP-1 itself, as has been reported for cultured HL-60 cells treated with phorbol 12-myristate 13-acetate (28). In an attempt to assign the oxidative stress response to any of the already characterized kinase pathways, we tested several pharmacological inhibitors for their ability to interfere with the H_2O_2 activation of IRP-1 in SLO-permeabilized cells. Following treatments with 100 μM of the kinase inhibitors herbimycin A and genistein (for protein tyrosine kinases); chelerythrine, staurosporine, and H7 (for protein kinase C); SB-203580 (for p38 mitogen-activated protein kinase); and rapamycin (for S6 kinase), the protein phosphatase inhibitor okadaic acid (1 μM), or phorbol 12-myristate 13-acetate (200 ng/ml), we could observe neither activation of IRP-1 nor a block of the H_2O_2-mediated activation of IRP-1 (data not shown). The lack of inhibition by okadaic acid was also observed previously *in vivo* (9), although variable results have been obtained with this drug using intact cells (7, 9). These preliminary data have to be interpreted with caution, because the effectivity of the above drugs in SLO-permeabilized cells was not monitored by inclusion of positive controls for the inhibitory effects of the respective compounds.

We suggest that the SLO-based cell-free system warrants consideration with regard to other oxidative stress-inducible proteins. Very recently, significant progress has been made in understanding the activation of the stress-inducible transcription factor NF-κB. A multiprotein complex seems to integrate a variety of environmental stimuli for activation of NF-κB by two kinases, IKKα and IKKβ, which phosphorylate and inactivate the inhibitor IκB (29–31). Because no cell-free system for studying NF-κB activation has been described so far, it will be interesting to see whether these responses can be reconstituted and dissected further in SLO-permeabilized cells.

Finally, the concept of "sensing" extracellular H_2O_2 by the IRE/IRP system may also have relevant implications for understanding the regulation of mammalian iron metabolism in pathophysiological situations, such as immune and inflammatory responses. Under these conditions, the respiratory burst of phagocytic polymorphonuclear and macrophage cells leads to the generation of reactive oxygen intermediates and to a dramatic increase in extracellular H_2O_2 (32). An IRP-1-mediated increase in cellular iron uptake via the transferrin receptor, or perhaps also via the recently described metal transporter DCT1, which is encoded by an mRNA containing an IRE motif in the 3′-untranslated region (33), may represent a cellular response to shift iron from the circulation into cells. In addition, increased intracellular iron in phagocytic cells may help to enhance the capacity of these cells to antagonize invading bacteria by increased generation of hydroxyl radicals in the phagosome through the Fenton reaction. Along similar lines, the inhibition of ferritin biosynthesis as a result of IRP-1 activation by oxidative stress may help to transiently sustain cytotoxic conditions in the phagosome.

We thank Dr. J. Krijnse-Locker for valuable advice concerning the usage of SLO, Dr. S. Mueller for determinations of k_{GO} and k_{cat} of the enzymes used in this study, and Dr. J. C. Lee (SmithKline Beecham) for the generous gift of SB-203580. This work was supported by the Deutsche Forschungsgemeinschaft (SFB 601).

1. Hentze, M. W. & Kühn, L. C. (1996) *Proc. Natl. Acad. Sci. USA* **93,** 8175–8182.
2. Rouault, T., Klausner, R. D. & Harford, J. B. (1996) *Translational Control of Ferritin* (Cold Spring Harbor Lab. Press, Plainview, NY), pp. 335–362.
3. Frishman, D. & Hentze, M. W. (1996) *Eur. J. Biochem.* **239,** 197–200.
4. Paraskeva, E. & Hentze, M. W. (1996) *FEBS Lett.* **389,** 40–43.
5. Beinert, H. & Kiley, P. (1996) *FEBS Lett.* **382,** 218–219.
6. Beinert, H., Holm, R. H. & Münck, E. (1997) *Science* **277,** 653–659.
7. Pantopoulos, K. & Hentze, M. W. (1995) *EMBO J.* **14,** 2917–2924.
8. Martins, E. A. L., Robalinho, R. L. & Meneghini, R. (1995) *Arch. Biochem. Biophys.* **316,** 128–134.
9. Pantopoulos, K., Weiss, G. & Hentze, M. W. (1996) *Mol. Cell. Biol.* **16,** 3781–3788.
10. Menotti, E., Henderson, B. R. & Kühn, L. C. (1998) *J. Biol. Chem.* **273,** 1821–1824.
11. Halliwell, B. & Gutteridge, J. M. C. (1990) *Methods Enzymol.* **186,** 1–85.
12. Gardner, P. R. & Fridovich, I. (1991) *J. Biol. Chem.* **266,** 19328–19333.
13. Gardner, P. R., Raineri, I., Epstein, L. B. & White, C. W. (1995) *J. Biol. Chem.* **270,** 13399–13405.
14. Rouault, T. A. & Klausner, R. D. (1996) *Trends Biochem. Sci.* **21,** 174–177.
15. Hentze, M. W. (1996) *Trends Biochem. Sci.* **21,** 282–283.
16. Pantopoulos, K., Mueller, S., Atzberger, A., Ansorge, W., Stremmel, W. & Hentze, M. W. (1997) *J. Biol. Chem.* **272,** 9802–9808.
17. Cairo, G., Castrusini, E., Minotti, G. & Bernelli-Zazzera, A. (1996) *FASEB J.* **10,** 1326–1335.
18. Meyer, M., Schreck, R. & Baeuerle, P. A. (1993) *EMBO J.* **12,** 2005–2015.
19. Nose, K., Shibanuma, M., Kikuchi, K., Kageyama, H., Sakiyama, S. & Kuroki, T. (1991) *Eur. J. Biochem.* **201,** 99–106.
20. Liu, X. & Thiele, D. J. (1996) *Genes Dev.* **10,** 592–603.
21. Hardwick, J. S. & Sefton, B. M. (1995) *Proc. Natl. Acad. Sci. USA* **92,** 4527–4531.
22. Pombo, C. M., Bonventre, J. V., Molnar, A., Kyriakis, J. & Force, T. (1996) *EMBO J.* **15,** 4537–4546.
23. Konishi, H., Tanaka, M., Takemura, Y., Matsuzaki, H., Ono, Y., Kikkawa, U. & Nishizuka, Y. (1997) *Proc. Natl. Acad. Sci. USA* **94,** 11233–11237.
24. Pantopoulos, K. & Hentze, M. W. (1995) *Proc. Natl. Acad. Sci. USA* **92,** 1267–1271.
25. Bhakdi, S., Tranum-Jensen, J. & Sziegoleit, A. (1985) *Infect. Immun.* **47,** 52–60.
26. Hentze, M. W., Rouault, T. A., Harford, J. B. & Klausner, R. D. (1989) *Science* **244,** 357–359.
27. Ohno, Y. & Gallin, J. I. (1985) *J. Biol. Chem.* **260,** 8438–8446.
28. Schalinske, K. L. & Eisenstein, R. S. (1996) *J. Biol. Chem.* **271,** 7168–7176.
29. Mercurio, F., Zhu, H., Murray, B. W., Shevchenko, A., Bennett, B. L., Li, J., Young, D. B., Barbosa, M., Mann, M., Manning, A. & Rao, A. (1997) *Science* **278,** 860–866.
30. Woronicz, J. D., Gao, X., Cao, Z., Rothe, M. & Goeddel, D. V. (1997) *Science* **278,** 866–869.
31. Zandi, E., Rothwarf, D. M., Delhase, M., Hayakawa, M. & Karin, M. (1997) *Cell* **91,** 243–252.
32. Baggiolini, M. & Thelan, M. (1991) *The Phagocytes and the Respiratory Burst* (Academic/Harcourt Brace Jovanovich, London), pp. 399–420.
33. Gunshin, H., Mackenzie, B., Berger, U. V., Gunshin, Y., Romero, M. F., Boron, W. F., Nussberger, S., Gollan, J. L. & Hediger, M. A. (1997) *Nature (London)* **388,** 482–488.